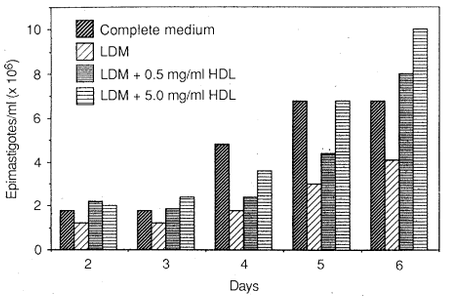

Fig. 4. Effect of HDL on the growth of *T. cruzi* epimastigotes (strain MV-13). Parasites were grown for the indicated time in a complete medium containing 10% fetal calf serum, in LDM, and in LDM reconstituted with human HDL at the indicated concentrations. The results shown are the average of duplicate tubes and representative of four experiments (standard deviation is less than 20% of the mean).

of its ability to inhibit neuraminidase activity of the infective trypomastigotes. Our observations support this concept (*27*). In this context, it is interesting that human HDL has been reported to have a specific lytic effect on trypomastigotes of the African trypanosome *T. brucei* and to be responsible for its host specificity (*28*). In view of these considerations, our working model is that HDL participates in the *T. cruzi* life cycle by promoting epimastigote multiplication in the insect vector and trypomastigote infection in the mammalian host. The results presented here raise the possibility that HDL may be one of the factors underlying the pathogenesis of Chagas' disease.

REFERENCES AND NOTES

1. M. E. A. Pereira, *Science* **219**, 1444 (1983).
2. ———, *J. Immunol. Methods* **63**, 25 (1983).
3. P. Libby, J. Alroy, M. E. A. Pereira, *J. Clin. Invest.* 77, 127 (1986).
4. M. E. A. Pereira and R. Hoff, *Mol. Biochem. Parasitol.* **20**, 183 (1986).
5. C. Cavalesco and M. E. A. Pereira, *J. Immunol.*, in press.
6. R. P. Prioli, I. Rosenberg, M. E. A. Pereira, *Proc. Natl. Acad. Sci. U.S.A.* **84**, 3097 (1987).
7. ———, in *Host-Parasite Cellular and Molecular Interactions in Protozoal Infections*, K. P. Chang and D. Snary, Eds. (NATO Advanced Science Institutes, Springer-Verlag, Heidelberg, 1987), p. 89.
8. U. K. Laemmli, *Nature (London)* **227**, 680 (1970).
9. Lipoprotein fractions [VLDL density, <1.006 g/ml; LDL density, 1.006 to 1.063 g/ml; and HDL density, 1.063 to 1.21 g/ml] were prepared by sequential flotation ultracentrifugation [V. N. Schumaker and D. L. Puppione, *Methods Enzymol.* **128**, 155 (1986)] with a Beckman 50.3 Ti rotor or by density gradient ultracentrifugation [J. L. Kelly and A. W. Kruski, *ibid.*, p. 170] with a Beckman SW 41 rotor at 40,000 rpm (280,000*g*), at 15°C for 48 hours.
10. H. Towbin, T. Staehelin, J. Gordon, *Proc. Natl. Acad. Sci. U.S.A.* 76, 4350 (1979).
11. Antibody to cruzin was elicited in rabbits as follows. Cruzin was purified from human plasma by polyethylene glycol precipitation, CM Affi-Gel Blue Sepharose (Bio-Rad) and Ultrogel AcA 34 (LKB) chromatography, and electrophoresis on SDS-polyacrylamide gel (*6*). Strips containing the cruzin bands (M_r 28,000) were excised, lyophilized, and ground to a fine powder with mortar and pestle. The powder containing approximately 30 μg of purified inhibitor was resuspended in 0.01*M* sodium phosphate–buffered saline (PBS), *p*H 7.2, and mixed with an equal volume of Freund's complete adjuvant for the first injection and with Freund's incomplete adjuvant for subsequent injections. Immune rabbit serum was collected after five injections 10 days apart. Preimmune and immune immunoglobulin G were purified by affinity chromatography on a protein A–Sepharose 4B column.
12. E. J. Schaefer and J. M. Ordovas, *Methods Enzymol.* **129**, 420 (1986).
13. E. J. Schaefer *et al.*, *J. Lipid Res.* **26**, 1089 (1985).
14. J. M. Ordovas *et al.*, *ibid.* **28**, 371 (1987).
15. Assays for inhibition of neuraminidase activity were performed as previously described (*6*). Water-soluble neuraminidase was harvested after the incubation of trypomastigotes for 72 hours at 4°C in the presence of serum-free medium containing protease inhibitors. Neuraminidase activity was assayed by incubating 50 μl of a fresh suspension of 10% human erythrocytes with 25 μl of the neuraminidase preparation for 2 hours at 37°C in a final volume of 100 μl of PBS. The erythrocyte suspension was then diluted to 2%. The degree of erythrocyte desialylation was determined by adding 25 μl of the suspension to a peanut lectin (PNA) solution diluted in microtiter plates. The hemagglutination titers were scored after incubation for 60 minutes at room temperature. Neuraminidase inhibition was assayed by incubating the proteins to be tested for inhibitory activity with neuraminidase for 60 minutes at 37°C before the addition of the red blood cells. One inhibition unit is defined as the amount of protein required to inhibit 50% of neuraminidase activity by the PNA hemagglutination method.
16. Human plasma apoA-I and apoB-100 were measured by a noncompetitive enzyme-linked immunosorbent assay (*17*). Polystyrene microtiter plates (Nunc Immunoplate 1, Denmark) were coated with affinity-purified polyclonal antibodies to apoA-I. Duplicate human plasma samples were diluted 1:3000 with PBS and added to designated wells in the microtiter plates, along with standards and controls obtained from the National Heart, Lung, and Blood Institute Lipid Research Clinics standardization program at the Centers for Disease Control (Atlanta, Georgia). After overnight incubation, immunopurified apoA-I polyclonal antibody conjugated to alkaline phosphatase was added. Color development was achieved with the addition of the substrate (0.1% *p*-nitrophenyl phosphate in 0.1*M* glycine). After 20 minutes at room temperature, the plates were read at 410 nm on a microtiter plate reader (Dynatech MR600), interfaced with an IBM XT microcomputer, and programmed with Immunosoft (Dynatech).
17. E. J. Schaefer *et al.*, *J. Lipid Res.* **23**, 850 (1982).
18. M. W. Hunkapiller, E. Lujan, F. Ostrander, L. E. Hood, *Methods Enzymol.* **91**, 227 (1983).
19. T. Gordon *et al.*, *Am. J. Med.* **62**, 707 (1977).
20. R. A. Norum *et al.*, *N. Engl. J. Med.* **306**, 1513 (1982).
21. J. F. Oram, J. J. Albers, M. C. Cheung, E. L. Bierman, *J. Biol. Chem.* **256**, 8348 (1981).
22. N. E. Miller, A. LaVille, D. Crook, *Nature (London)* **314**, 109 (1985).
23. P. Libby, P. Miao, J. M. Ordovas, E. J. Schaefer, *J. Cell. Physiol.* **24**, 1 (1985).
24. Epimastigote growth medium consists of brain-heart infusion supplemented with 10% fetal calf serum [M. E. A. Pereira and D. Moss, *Mol. Biochem. Parasitol.* **15**, 95 (1985)]. The LDM was prepared in the same way except that the fetal calf serum was subjected to ultracentrifugation on a KBr gradient to remove lipoproteins (*9*); LDM was reconstituted by addition of human HDL purified as in (*9*).
25. Z. Brener, *Annu. Rev. Microbiol.* **27**, 349 (1973).
26. R. P. Prioli, I. Rosenberg, S. Shivakumar, M. E. A. Pereira, in preparation.
27. R. P. Prioli, I. Rosenberg, M. E. A. Pereira, in preparation.
28. M. R. Rifkin, *Proc. Natl. Acad. Sci. U.S.A.* **75**, 3450 (1978).
29. H. N. Brewer *et al.*, *Biochem. Biophys. Res. Commun.* **80**, 623 (1978).
30. C. C. Shoulders *et al.*, *Nucleic Acids Res.* **11**, 2827 (1983).

31. We thank G. Fasman and J. Benner for help in verifying the amino acid homology and M. Sela and J. Sharon for critical reading of the manuscript and helpful suggestions. Supported by NIH grants AI 18102 and HL 35243, and the United Nations Development Program/World Bank/World Health Organization Special Program for Research and Training in Tropical Diseases (M.E.A.P.), NIH postdoctoral fellowship AI 07380 (I.R.), contract 53-3K-06 from the U.S. Department of Agriculture Research Service, and by a grant from the Rockefeller Foundation to the Division of Geographic Medicine.

26 June 1987; accepted 14 October 1987

Effect of Membrane Potential Changes on the Calcium Transient in Single Rat Cardiac Muscle Cells

MARK B. CANNELL,* JOSHUA R. BERLIN, WILLIAM J. LEDERER

The mechanism that links membrane potential changes to the release of calcium from internal stores to cause contraction of cardiac cells is unclear. By using the calcium indicator fura-2 under voltage-clamp conditions, changes in intracellular calcium could be monitored in single rat ventricular cells while controlling membrane potential. The voltage dependence of the depolarization-induced increase in intracellular calcium was not the same as that of the calcium current (I_{si}), which suggests that only a small fraction of I_{si} is required to trigger calcium release from the sarcoplasmic reticulum. In addition, sarcoplasmic reticulum calcium release may be partly regulated by membrane potential, since repolarization could terminate the rise in intracellular calcium. Thus, changes in the action potential will have immediate effects on the time course of the calcium transient beyond those associated with its effects on I_{si}.

STUDIES ON CARDIAC MUSCLE HAVE shown that the amplitude of the calcium current (I_{si}) and the strength of contraction are closely linked (*1*), supporting the idea that the Ca^{2+} flux across the surface membrane during I_{si} directly trig-

M. B. Cannell, Department of Pharmacology, University of Miami School of Medicine, Miami, FL 33136.
J. R. Berlin and W. J. Lederer, Department of Physiology, University of Maryland School of Medicine, Baltimore, MD 21201.

*To whom correspondence should be addressed.

gers and regulates the release of Ca^{2+} from the sarcoplasmic reticulum (SR) (*2*). However, the change in intracellular Ca^{2+} ($[Ca^{2+}]_i$) that activates contraction is transient, so that force development will depend on the time course of the $[Ca^{2+}]_i$ transient as well as the nonlinear Ca^{2+}-force relation (*3*). Thus force is, at best, only a qualitative measure of $[Ca^{2+}]_i$, and the relation between I_{si} and $[Ca^{2+}]_i$ may not have been characterized by tension measurements.

We have directly addressed this issue by recording $[Ca^{2+}]_i$ transients from voltage-clamped single rat ventricular cells with the fluorescent Ca^{2+} indicator fura-2 (*4*). The fura-2 was introduced into the cell by including the potassium salt of fura-2 in the patch electrode filling solution. Although introducing fura-2 into the cell in this way is more difficult than using the membrane permeant acetoxymethylester form of fura-2 (fura-2 AM), it ensures that the recorded fluorescent signals are uncontaminated by partially deesterified forms of fura-2 AM (*5*) and by fura-2 AM entering membrane bound organelles. After isolation (*6*), cells were transferred to the experimental chamber (*7*) mounted on the stage of a modified inverted microscope (*8*). The bathing solution contained 145 m*M* NaCl, 4 m*M* KCl, 1 m*M* $MgCl_2$, 1 m*M* $CaCl_2$, 10 m*M* glucose, 0.03 m*M* tetrodotoxin, and 10 m*M* Hepes (*p*H 7.4, 35°C). Cells could be illuminated by ultraviolet (UV) light via an epifluorescence illuminator constructed from fused silica components and a 100-W mercury arc lamp. Illumination with UV light at a wavelength of 340 or 380 nm was selected by 10-nm interference filters (*8*). Quiescent cells were voltage-clamped with a single patch electrode (*9*). The patch-electrode filling solution contained an intracellular salt solution (*10*) that included 30 μ*M* fura-2 (K^+ salt) (*11*). Fluorescence of the cell at 505 nm was recorded from a region of the cell about 10 μm in diameter with a photomultiplier tube. $[Ca^{2+}]_i$ was estimated by dividing fura-2 fluorescence (at 505 nm, after background autofluorescence subtraction) obtained with 340-nm illumination by that obtained with 380-nm illumination (*4*). This division gives a "fluorescence ratio" that can be converted to Ca^{2+} concentrations with an in vitro calibration curve (Fig. 1A) (*4, 12, 13*).

Depolarization of the cell by a voltage-clamp step produced changes in fluorescence at both illumination wavelengths (Fig. 1B); fluorescence (at 505 nm) transiently increased while the cell was illuminated with 340-nm light and decreased while the cell was illuminated at 380 nm. These changes in fluorescence would be expected from a transient increase in $[Ca^{2+}]_i$ (*4*) (Fig. 1A). Although in opposite directions, the time course of the transient at each illumination wavelength was similar and free from detectable movement artifacts (*14*).

The fluorescence signal changes rapidly at first and then more slowly for the remainder of the depolarizing pulse. The rate of change of the fluorescence signal during the rising phase of the transient (about 100 sec^{-1}) may be limited by the speed of response of fura-2 (*15*). However, once the rapid phase of the transient is complete, the dye signal should give a reasonable estimate of the time course of the underlying $[Ca^{2+}]_i$ transient (Fig. 1B). About 3 msec after depolarization $[Ca^{2+}]_i$ started to increase and reached its peak value at about 40 msec. Upon repolarization $[Ca^{2+}]_i$ declined with a half time of about 50 msec and was still elevated more than 300 msec after repolarization. Thus the duration of the $[Ca^{2+}]_i$ transient is at least as long as the twitch. Although $[Ca^{2+}]_i$ transients measured by aequorin generally appear briefer than this (*16*), the inability to resolve resting levels of $[Ca^{2+}]_i$ with aequorin and the nonlinear dependence of aequorin light on Ca^{2+} (*17*) lead us to believe that there are no fundamental differences between the $[Ca^{2+}]_i$ transient mea-

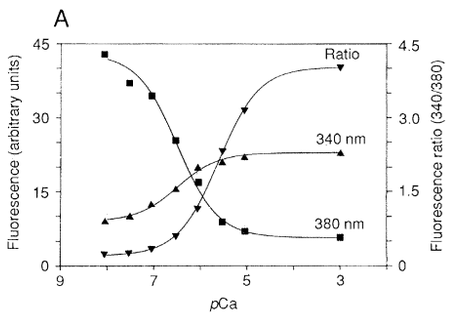

Fig. 1. (**A**) An in vitro calibration curve for fura-2 fluorescence measured at 505 nm. Fluorescence intensity during illumination with 340-nm (▲) and 380-nm light (■) and the resulting ratio (▼) of fluorescence intensities (*4, 12*) are displayed as a function of Ca^{2+} concentration. The calibration solution contained 140 m*M* KCl, 1 m*M* $MgCl_2$, 5 m*M* EGTA (K^+ salt), 10 μ*M* fura-2 (K^+ salt), 20 m*M* Pipes (*p*H 7.2). $CaCl_2$ was added to set the level of free Ca^{2+} concentration (dissociation constant of EGTA, 294 n*M*). Fluorescence measurements were performed at 35°C on the same apparatus used for experiments (**B**) Traces show (from top to bottom): membrane potential, membrane current, fluorescence at 505 nm during illumination with 380-nm and 340-nm light, and $[Ca^{2+}]_i$. The fluorescence records at each illumination wavelength are displayed by using an arbitrary scale. To estimate $[Ca^{2+}]_i$, the fluorescence record obtained during 340-nm illumination was divided by the fluorescence record at 380 nm after subtracting autofluorescence backgrounds at each wavelength. $[Ca^{2+}]_i$ was then determined from this ratio of fluorescence intensities with the in vitro calibration curve in (A).

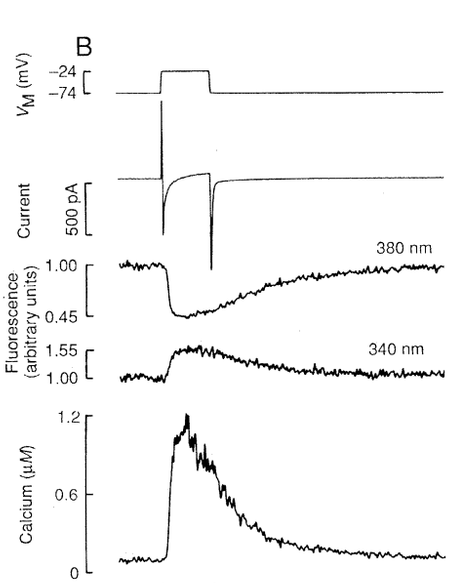

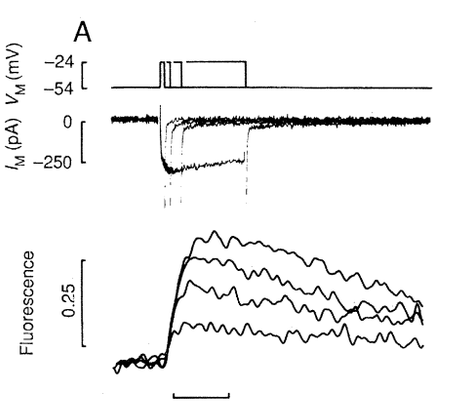

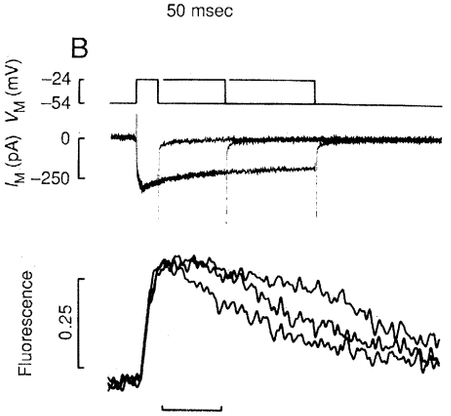

Fig. 2. Effect of depolarization duration on the time course of the Ca^{2+} transient. The cell was depolarized from −54 to −24 mV for 100 msec every 1.5 seconds. Every fourth depolarization, the duration of the depolarizing pulse was varied between 5 and 320 msec. (**A**) Depolarizing pulses of 5-, 10-, 20-, and 80-msec duration. (**B**) Pulses of 40-, 160-, and 320-msec duration. The upper record in each panel shows membrane potential. The middle record shows membrane current corrected for capacity and leak currents. The lower record shows changes in fluorescence measured at 505 nm during illumination with 380-nm light. The fluorescence record was low-pass filtered (8-pole Bessel, −6 dB at 80 Hz).

sured by aequorin and those reported here. In addition, the estimate of peak $[Ca^{2+}]_i$ obtained here is similar to that estimated from aequorin transients in rat papillary muscle under similar conditions (*18*).

The effect of changing the duration of depolarizing pulses that gave nearly maximal transient amplitudes is shown in Fig. 2. Similar results were observed in ten other cells. Three features of this figure are notable: (i) Repolarization during the rising phase of the transient abbreviates the rise in $[Ca^{2+}]_i$. (ii) After about 40 msec $[Ca^{2+}]_i$ starts to decline from the peak level even if the membrane is still depolarized. [A similar result has been observed in aequorin-injected Purkinje fibers under voltage clamp (*19, 20*).] (iii) The rate of decline of $[Ca^{2+}]_i$ is increased if the membrane is repolarized. In addition, with long depolarizing pulses $[Ca^{2+}]_i$ does not return to resting levels but is maintained at an elevated level and in some experiments increased again. This latter feature is similar to the voltage- which sodium-dependent changes in resting $[Ca^{2+}]_i$ which tonic tension observed in Purkinje fibers and may be due to the Na^{2+}-Ca^{2+} exchange mechanism (*20, 21*).

It has been suggested that the release of Ca^{2+} by the SR is regulated by I_{si} and not by the change in membrane potential per se (*22*). In this "calcium-induced calcium release" (CICR) mechanism, Ca^{2+} entering via I_{si} binds to an activator site that causes the SR Ca^{2+} release channel to open. The regenerative nature of this mechanism is suppressed by Ca^{2+} slowly binding to an inhibitory site that stops Ca^{2+} release (*23*). The depression of the rising phase of the $[Ca^{2+}]_i$ transient by rapid repolarization might be due to the more rapid increase of $[Ca^{2+}]_i$ near the regulatory sites upon repolarization (thereby inhibiting release more rapidly). During the few milliseconds that I_{si} takes to deactivate after repolarization, an increase in Ca^{2+} influx would be expected from the increase in the electrochemical gradient for Ca^{2+} entry. However, repolarizing from −24 to −54 mV would not be expected to increase the Ca^{2+} influx rate by more than about 20% (because the Nernst potential for Ca^{2+} is about +90 mV). It is difficult to reconcile such a moderate and short-term increase in Ca^{2+} influx with such a profound depression of release, since depolarizations that give a larger I_{si} (see below) increase the amplitude of the $[Ca^{2+}]_i$ transient. Alternatively, the occupancy of activator site might be decreased by the cessation of the Ca^{2+} influx, so that Ca^{2+} release is inhibited. However, when repolarization stops the rise in $[Ca^{2+}]_i$, Ca^{2+} is already being released by the SR so that the occupancy of the activator sites will depend on the relative contributions of I_{si} and SR Ca^{2+} fluxes to the local $[Ca^{2+}]_i$ around the SR release sites. Consideration of the amplitude of the I_{si} and the rate of change of the fura-2 fluorescence signal suggests that the Ca^{2+} flux from the SR is at least an order of magnitude greater than that due to I_{si} (*24*). Thus once initiated, SR Ca^{2+} release should dominate $[Ca^{2+}]_i$ near the release sites and removal of the I_{si} Ca^{2+} flux (by repolarization) should not lead to a large decrease in the occupancy of the activator sites. If CICR alone cannot account for why repolarization abbreviates the rise in $[Ca^{2+}]_i$, then our data raise the possibility that repolarization may also directly inhibit SR Ca^{2+} release.

The voltage dependence of the $[Ca^{2+}]_i$ transient and Ca^{2+} currents is illustrated in Fig. 3. I_{si} activates at about −40 mV and reaches half maximal amplitude at −22 mV. I_{si} reaches a peak at about −10 mV, and further depolarization results in a decrease of the amplitude of I_{si} (because of the decreasing driving force for Ca^{2+} entry). These characteristics of I_{si} are similar to those reported elsewhere (*25*). However, peak $[Ca^{2+}]_i$ has a very different voltage dependence. Detectable increases in $[Ca^{2+}]_i$ occur when the cell is depolarized to −50 mV, while a half-maximal increase in $[Ca^{2+}]_i$ occurs at about −38 mV. With larger depolarizations, the peak $[Ca^{2+}]_i$ reaches a maximum that becomes relatively voltage insensitive over the range −20 to 20 mV. Depolarization beyond about 30 mV results in a decrease in the amplitude of the $[Ca^{2+}]_i$ transient during the pulse and the development of an additional $[Ca^{2+}]_i$ transient that occurs on repolarization. The observation that the voltage dependence of peak $[Ca^{2+}]_i$ is quite different from that of I_{si} [in six experiments, I_{si} was half maximal at −17.8 ± 1.4 mV, whereas the $[Ca^{2+}]_i$ transient was half maximal at −30.3 ± 1.7 mV (mean ± SEM)] suggests that the increases in $[Ca^{2+}]_i$ that we have recorded are not simply a reflection of the contribution of I_{si} to $[Ca^{2+}]_i$. Thus, the SR Ca^{2+} release

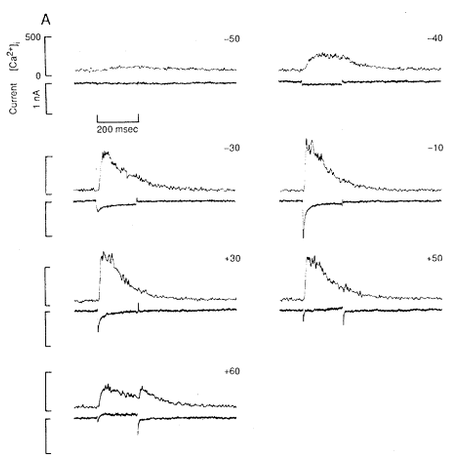

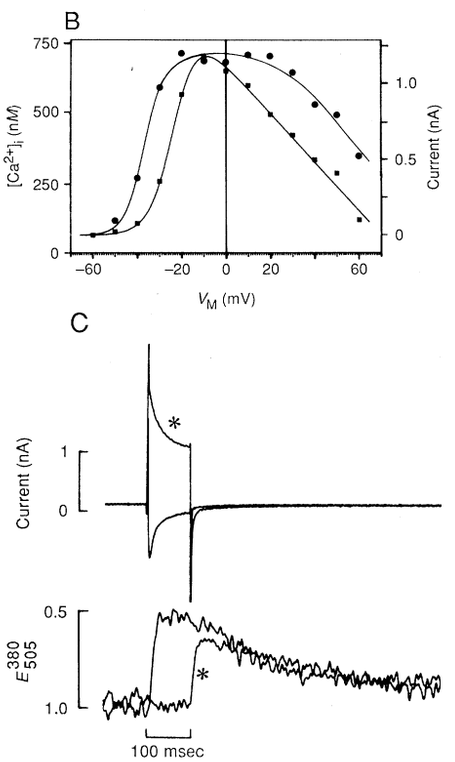

Fig. 3. An example of the voltage dependence of the Ca^{2+} transient and I_{si}. (**A**) The changes in $[Ca^{2+}]_i$ (top) and I_{si} (bottom) elicited by 200-msec test depolarizations to various potentials (shown on the right of each panel). The test depolarization was given after a train of constant amplitude depolarizations (at 1 Hz) to place the cell in the same state before each test pulse. The currents shown are difference currents obtained by subtracting records obtained in the presence of a calcium channel blocker (25 μ*M* D-600) from control records (*30*). Calibration scales are the same for each panel. Note the graded increase in both the rate of rise of $[Ca^{2+}]_i$ and the peak $[Ca^{2+}]_i$ reached during the depolarization. In addition, depolarization to −50 and −40 mV elicits an increase in $[Ca^{2+}]_i$ without activating a time-dependent inward current. (**B**) Depolarization potential as a function of peak $[Ca^{2+}]_i$ (circles) and peak I_{si} (squares) for the experiment in (A). A modified Boltzmann equation (which takes account of the variation in driving force on the activation of the current) has been fitted to the current data: $I_{Ca} \alpha (E_{si}-V_m)/1 + \exp[-(V_m-V_h)/k]$, where E_{si} is the extrapolated reversal potential for the current (+70 mV), V_m is the membrane potential, V_h is the half maximal activation potential (−23 mV), and k is the slope factor (5.4 mV). The curve through the $[Ca^{2+}]_i$ data points was drawn by eye. (**C**) Effect of depolarization to very positive potentials. Superimposed records of membrane currents (upper panel) and fluorescence changes (bottom panel) (excitation, 380 nm; emission, 505 nm) associated with a 100-msec depolarization to +10 and +100 mV (designated with an asterisk). Membrane current and fluorescence changes at +10 mV are similar to those in (A), but depolarization to +100 mV (*) results in no $[Ca^{2+}]_i$ transient during the pulse and a clear transient on repolarization.

system was functional and not blocked by the injection of fura-2. In addition, if I_{si} does trigger the release of Ca^{2+} from the SR (*2*), then only a small fraction of I_{si} is required to initiate Ca^{2+} release (*26*). The observation that increasing activation of I_{si} (Between −25 and ø mV) has only a small effect on peak $[Ca^{2+}]_i$ supports the suggestion that, in rat ventricular cells, the increase in $[Ca^{2+}]_i$ elicited by depolarization is principally due to Ca^{2+} release from the SR and Ca^{2+} influx via I_{si} is a relatively minor component (*27*).

At very positive potentials, there was no Change in $[Ca^{2+}]_i$ during the pulse and a subsequent $[Ca^{2+}]_i$ transient occurred on repolarization (Fig. 3C). This result suggests that Ca^{2+} entry via the Na^{2+}-Ca^{2+} exchange mechanism during the depolarizing pulse is insufficient to activate Ca^{2+} release from the SR under these conditions (assuming that CICR is the mechanism of Ca^{2+} release). The repolarization transient could be explained by the tail Ca^{2+} current activating Ca^{2+} release from the SR by the CICR mechanism. Alternatively, if the SR Ca^{2+} release channel rapidly enters an inactivated state at these positive potentials (so that no transient occurs during the pulse), then the repolarization transient could be explained by the return of the channel through the open state. It is also possible that Ca^{2+} entering during the depolarizing pulse is taken up by the SR (which could also help explain the lack of an appreciable change in $[Ca^{2+}]_i$ during the pulse) and that this causes the SR to enter a "Ca^{2+} overload" state (*28*) so that spontaneous Ca^{2+} release occurs once inhibition of Ca^{2+} release is relieved by repolarization.

Our results are compatible with both the CICR mechanism and a voltage-dependent SR Ca^{2+} release mechanism. However, the effect of rapid repolarization appears more easily explained by voltage directly affecting Ca^{2+} release than by CICR. Thus, Ca^{2+} release may be mediated by a mechanism that requires a Ca^{2+} influx but which may also be modulated by changes in voltage directly.

Because maintained depolarization slows the return of $[Ca^{2+}]_i$ to resting levels, changes in the duration of the action potential should affect the time course of the $[Ca^{2+}]_i$ transient. Such changes do not arise from changes in the amount of Ca^{2+} available for release from the SR (because they can be observed on the first long pulse in a train of depolarizations) and represent an additional regulatory mechanism for force production. Thus (for example), interventions that increase the duration of the action potential will tend to increase force production immediately by increasing the duration of the $[Ca^{2+}]_i$ transient. Changes in Ca^{2+} influx during the action potential will further augment subsequent Ca^{2+} release by increasing the amount of releasable Ca^{2+} stored within the SR.

Note added in proof: Barcenas-Ruiz and Wier (*29*) have recently reported the voltage dependence of fura-2 fluorescence transients in guinea pig cardiac myocytes. Their data suggest that fluorescence transients and I_{si} may activate over the same range of membrane potentials. While this different result may have arisen from their choice of resting membrane potential, it is also possible that there are species differences between rat and guinea pig cardiac myocytes.

REFERENCES AND NOTES

1. G. W. Beeler, Jr., and H. Reuter, *J. Physiol. (London)* **207**, 211 (1970); R. Ochi and W. Trautwein, *Pfluegers Arch.* **323**, 187 (1971); W. New and W. Trautwein, *ibid.* **334**, 24 (1972); W. Trautwein, T. F. McDonald, O. Tripathi, *ibid.* **354**, 55 (1975); G. Isenberg and U. Klockner, *ibid.* **395**, 30 (1982); B. London and J. W. Krueger, *J. Gen. Physiol.* **88**, 475 (1986).
2. M. Morad and Y. Goldman, *Prog. Biophys. Mol. Biol.* **27**, 257 (1973); W. R. Gibbons and H. A. Fozzard, *J. Gen. Physiol.* **65**, 367 (1975); B. London and J. W. Krueger, *ibid.* **88**, 475 (1986).
3. D. T. Yue, E. Marban, W. G. Wier, *J. Gen. Physiol.* **87**, 223 (1986).
4. G. Grynkiewicz, M. Poenie, R. Y. Tsien, *J. Biol. Chem.* **260**, 3440 (1985).
5. M. Scanlon, D. A. Williams, F. S. Fay, *J. Gen. Physiol.* **88**, 52a (1986).
6. T. Powell, D. A. Terrar, V. W. Twist, *J. Physiol. (London)* **302**, 131 (1980); J. R. Hume and W. R. Giles, *J. Gen. Physiol.* **78**, 19 (1981); G. Isenberg and U. Klockner, *Pfluegers Arch.* **395**, 30 (1982).
7. M. B. Cannell and W. J. Lederer, *Pfluegers Arch.* **406**, 536 (1986).
8. W. G. Wier, M. B. Cannell, J. R. Berlin, E. Marban, W. J. Lederer, *Science* **235**, 325 (1987).
9. O. P. Hamill, A. Marty, E. Neher, B. Sakmann, F. J. Sigworth, *Pfluegers Arch.* **391**, 85 (1981).
10. The patch-pipette filling solution contained 83 m*M* potassium glutamate, 20 m*M* CsCl, 5 m*M* $MgCl_2$, 5 m*M* glucose, 3.3 m*M* adenosine triphosphate (K^+ salt), 3.75 m*M* phosphocreatine (Na^{2+} salt), 8.3 m*M* phosphocreatine (Tris salt), 0.1 m*M* DL-dithiothreitol (DTT), creatine phosphokinase (30 U/ml), 0.03 m*M* fura-2 (K^+ salt), and 30 m*M* Pipes (piperazine-*N*-*N*′-bis[2-ethane-sulfonic acid]), *p*H 7.2.
11. Patch electrode resistances were 1 to 3 Mohm, and the liquid junction potential between the patch filling solution and the bathing solution was measured (4 mV) and subtracted from the voltage records. After the electrode was sealed onto the surface of a cell, the background autofluorescence of the cell was measured to enable accurate determination of the fluorescence of the injected fura-2. After breaking the patch of membrane under the patch electrode, the diffusion of fura-2 into the cell (as measured by increasing fluorescence) often occurred spontaneously. However, positive pressure applied to the back of the patch electrode was used occasionally to facilitate loading. Although some buffering of $[Ca^{2+}]_i$ would be expected from this concentration of fura-2 [M. P. Timmerman and C. C. Ashley, *FEBS Lett.* **209**, 1 (1986)], three pieces of evidence suggest that the buffering of $[Ca^{2+}]_i$ by 30 μ*M* fura-2 is not a serious problem. (i) During the time (typically 5 minutes) that it takes the fura-2 in the pipette to come into equilibrium with the cell contents, there is little or no change in the peak level of $[Ca^{2+}]_i$ reached in response to constant amplitude depolarizing pulses. (ii) Cardiac cells contain Ca^{2+} buffers (such as troponin and Ca^{2+} binding sites on calmodulin) at a concentration of several hundred micromolar, so that the extra buffering arising from the fura-2 is only a small fraction of the total buffering power of the cell [London and Krueger (*1*) reported that 800 μ*M* EGTA did not abolish contraction in cardiac myocytes]. (iii) The time course of the $[Ca^{2+}]_i$ transient that we measured is very similar to that reported for aequorin (see above). The patch pipette also acts as a source and sink for Ca^{2+} within the cell. Because it takes several minutes for the contents of the pipette to come into equilibrium with the cytoplasm, it is clear (from the time course of the Ca^{2+} transient) that cell Ca^{2+} metabolism can alter the level of $[Ca^{2+}]_i$ at least 100 times faster than the pipette. Thus the buffering of cell Ca^{2+} by the pipette is unlikely to be a problem. Furthermore, the pipette is too far from the measurement spot (typically between 10 and 20 μm) for an appreciable amount of Ca^{2+} to diffuse from the measurement site to the pipette within the time scale of the twitch. This is because the diffusion coefficient for Ca^{2+} in the cytoplasm is approximately 1/50 of that in free solution (because of the presence of nondiffusible Ca^{2+} binding sites with fast kinetics).
12. D. A. Williams, K. E. Fogarty, R. Y. Tsien, F. S. Fay, *Nature (London)* **318**, 558 (1985).
13. The calculation of $[Ca^{2+}]_i$ by this method assumes that the properties of fura-2 inside the cell are the same as in the calibration solution. However, the effect of the intracellular environment on fura-2 is not known. Williams *et al.* (*12*) found that the calibration curve obtained in vitro was similar to that obtained for fura-2 inside smooth muscle cells. Furthermore, the accuracy of the calibration curve in our experiments may be improved by the partial dialysis of the intracellular medium by the patch electrode filling solution. Despite these considerations, we have included calibration information needed to recalculate the levels of $[Ca^{2+}]_i$ should the properties of fura-2 inside cells prove different from those in our calibration solution. In spite of these concerns, any errors in the exact values of $[Ca^{2+}]_i$ reported by fura-2 do not affect our conclusions.
14. The maximum cell shortening observed in these experiments was estimated visually to be about 10%. Assuming a constant cell volume, this shortening would correspond to about a 5% increase in cell thickness and dye fluorescence at a single wavelength. However, such changes in fluorescence associated with shortening were not detected. This may be because the depth of focus of the microscope was less than the thickness of the cell so that fluorescence was recorded from an optical section of constant thickness. In addition, fluorescence was recorded from a region of the cell near the clamping electrode, which pinned the cell to the bottom of the chamber. The pressure exerted on the cell surface by the electrode would tend to minimize cell movement and changes in cell thickness in the area around it.
15. The kinetics of Ca^{2+} binding to fura-2 have not been measured at 35°C. At 20°C the association rate constant is $5 \times 10^8 M^{-1}$ sec^{-1} and the dissociation rate constant is 84 sec^{-1} for Ca^{2+} binding [A. P. Jackson, M. P. Timmerman, C. R. Bagshaw, C. C. Ashley, *FEBS Lett.* **216**, 35 (1987)] so that at 200 n*M* $[Ca^{2+}]$ the apparent rate constant for the fura-2 reaction would be about 180 sec^{-1}. Although the rate constants of Ca^{2+} binding to fura-2 reaction may be increased at the experimental temperature used in our study, the overall rate of the fura-2 reaction is not large enough to allow the possible kinetic distortion of the rising phase of the $[Ca^{2+}]_i$ transient to be ignored.
16. D. G. Allen and S. Kurihara, *J. Physiol. (London)* **327**, 79 (1982).
17. J. R. Blinks, W. G. Wier, P. Hess, F. G. Prendergast, *Prog. Biophys. Mol. Biol.* **40**, 1 (1982).
18. D. G. Allen and S. Kurihara, *Eur. Heart J.* **1A**, 5 (1980).
19. W. G. Wier and G. Isenberg, *Pfluegers Arch.* **392**, 284 (1982); D. A. Eisner and M. Valdeolmillos, *J. Physiol. (London)* **375**, 269 (1986).
20. M. B. Cannell, D. A. Eisner, W. J. Lederer, M. Valdeolmillos, *ibid.* **381**, 193 (1986).
21. D. A. Eisner, W. J. Lederer, R. D. Vaughan-Jones, *ibid.* **335**, 723 (1984).
22. A. Fabiato, *J. Gen. Physiol.* **85**, 291 (1985); B.

London and J. W. Krueger, *ibid.* **88**, 475 (1986).
23. A. Fabiato, *ibid.* **85**, 247 (1985).
24. Assuming a cell volume of 30 pl, a Ca^{2+} current of 0.5 nA would correspond to an increase in $[Ca^{2+}]_i$ of 0.08 μM/msec. The fura-2 Ca^{2+} transient suggests that $[Ca^{2+}]_i$ is changing at not less than 0.03 μM/msec at 5 msec after depolarization. Assuming that the free Ca^{2+} represents 2% of the total Ca^{2+} released (the remainder being rapidly bound), then intracellular calcium must be rising at about 1.5 μM/msec. Thus the rate of Ca^{2+} release by the SR is at least an order of magnitude greater than the flux arising from the Ca^{2+} current.
25. R. S. Kass and M. C. Sanguinetti, *J. Gen. Physiol.* **84**, 705 (1984); H. Matsuda and A. Noma, *J. Physiol. (London)* **357**, 553 (1984); I. R. Josephson *et al.*, *Circ. Res.* **54**, 144 (1984).
26. There is increasing evidence for more than one Ca^{2+} channel type in various tissues. In atrial cells, B. P. Bean [*J. Gen. Physiol.* **86**, 1 (1985)] showed a low threshold Ca^{2+} channel that activated at about −40 mV. B. Nilius, P. Hess, J. B. Lansman, and R. W. Tsien [*Nature (London)* **316**, 443 (1985)] described a T-type Ca^{2+} channel in guinea pig ventricular muscle. Although our Ca^{2+} currents do not exhibit current components that might be ascribed to T-type Ca^{2+} channels, it is possible that they were undetected because we measured the D-600–sensitive current. It is not known whether D-600 blocks T-type Ca^{2+} channels. If this type of channel were present in rat ventricular cells, it might provide the Ca^{2+} needed to activate the CICR mechanism in the voltage range where we first detect changes in $[Ca^{2+}]_i$.
27. G. Isenberg, A. Beresewicz, D. Mascher, F. Valenzuela, *Basic Res. Cardiol. (Suppl. 1)* **80**, 117 (1985).
28. A. Fabiato and F. Fabiato, *J. Physiol. (London)* **249**, 469 (1975); C. H. Orchard, D. A. Eisner, D. G. Allen, *Nature (London)* **304**, 735 (1983); W. G. Wier *et al.*, *Proc. Natl. Acad. Sci. U.S.A.* **80**, 7367 (1983).
29. L. Barcenas-Ruiz and G. W. Wier, *Circ. Res.* **61**, 148 (1987).
30. The D-600 was diluted from a stock solution (100 mM in ethanol). A concentration of 25 μM is about ten times that needed to block I_{si} in other cardiac preparations under similar conditions [K. S. Lee and R. W. Tsien, *Nature (London)* **297**, 498 (1982); T. F. McDonald, D. Pelzer, W. Trautwein, *J. Physiol. (London)* **352**, 217 (1984)].
31. Supported by NIH grant HL25675 (W.J.L.) and by grants from the American Heart Association and the Maryland Heart Association to M.B.C., J.R.B., and W.J.L. W.J.L. is an Established Investigator of the American Heart Association and its Maryland Affiliate. M.B.C. was supported by a Young Investigatorship of the Maryland Affiliate of the American Heart Association. We thank K. MacEachern for assistance in manuscript preparation.

23 April 1987; accepted 8 September 1987

Technical Comments

Virus-Induced Increases in Plasma Corticosterone

E. M. Smith *et al.* (*1*) reported results consistent with the hypothesis that cells of the immune system are able to initiate an adrenocortical stress response by releasing adrenocorticotropin (ACTH), indicating a "lymphoid-adrenal axis." The basis for their hypothesis was the observation that injection of hypophysectomized mice with Newcastle disease virus (NDV) elevated plasma concentrations of corticosterone, together with their earlier observation that lymphocytes in vitro responded to NDV exposure by releasing ACTH (*2*).

Smith *et al.* report testing the completeness of hypophysectomy by visual inspection of the sella tursica; functional testing by the stress of cold-water immersion was performed in a separate group of mice that did not receive NDV. This is important because Moldow and Yalow (*3*) have shown that, unless all corticotrophic tissue is removed, cells may survive, multiply, and eventually restore full corticotrophic function. We have repeated the experiments of Smith *et al.* and obtained somewhat different results in hypophysectomized mice in which the completeness of hypophysectomy was verified by prior restraint or CRF administration.

In our experiments (*4*), each mouse was tested for the completeness of hypophysectomy (with restraint) and for adequate adrenocortical function (by injecting ACTH) before we administered NDV. Three days after hypophysectomy, each mouse was placed in a restraining device for 60 minutes, after which approximately 150 μl of blood was collected from the tail vein (in 5 to 15 minutes). On the next day, each mouse was injected subcutaneously with $ACTH_{1\text{-}24}$ (Organon, 1 μg/g), and tail blood was again sampled 30 minutes later. On the fifth day after hypophysectomy, mice were intraperitoneally injected with NDV (0.3 ml) or control allantoic fluid (*5*) and were decapitated 8 hours after injection to collect trunk blood. Plasma corticosterone was assayed by radioimmunoassay (*6*).

We present in Table 1 the combined results of two separate experiments with the same design (*7*). Hypophysectomized mice did not show elevated plasma corticosterone concentrations after restraint. ACTH-induced concentrations of plasma corticosterone were slightly lower in hypophysectomized mice than in sham-operated controls, consistent with a small loss of adrenocortical sensitivity. As would be expected after removal of the pituitary, the plasma of hypophysectomized mice contained lower concentrations of corticosterone than did sham-operated controls, whether or not they were injected with NDV. NDV-injected sham-operated mice showed statistically significant elevations of plasma corticosterone relative to vehicle-injected controls. In these two experiments, there was a small increase in the plasma corticosterone concentrations of hypophysectomized mice injected with NDV as compared with vehicle, but this effect was not statistically significant. Thus hypophysectomy prevented the

Table 1. Plasma corticosterone concentrations (nanograms per milliliter) after NDV administration to hypophysectomized or sham-operated mice. Three days after hypophysectomy mice were tested for completeness of hypophysectomy by restraining them for 60 minutes and collecting a sample of blood from the tail vein. Adrenocortical responsiveness was tested the next day 30 minutes after subcutaneous injection of $ACTH_{1\text{-}24}$ (1 μg/g). On the fifth day after hypophysectomy, mice were injected intraperitoneally with 0.3 ml of NDV (750 hemagglutination units) or with control allantoic fluid 8 hours before trunk blood was collected for assay of corticosterone by radioimmunoassay. Three hypophysectomized mice displaying plasma corticosterone concentrations greater than 50 ng/ml after restraint and two exhibiting corticosterone concentrations less than 100 ng/ml after ACTH were excluded from the hypophysectomized group. The results after NDV injection were similar whether or not any mice were excluded.

Treatment-injection	Plasma corticosterone concentrations (ng/ml)			
	N	Prior restraint	ACTH injection	NDV injection
Sham-operated				
Vehicle	17	284 ± 19	409 ± 25	85 ± 13
NDV	17	284 ± 23	448 ± 34	167 ± 21*
Hypophysectomized				
Vehicle	17	19 ± 3	327 ± 38†	21 ± 5
NDV	16	24 ± 4	336 ± 39†	37 ± 9

*NDV injection caused a statistically significant elevation of plasma corticosterone compared with that in the vehicle-injected group in sham-operated mice [$t(df = 32) = 3.29$, $P < 0.005$], but not in hypophysectomized mice. †The plasma concentrations of corticosterone after ACTH injection were significantly lower in the hypophysectomized than in the sham-operated mice [$t(df = 65) = 2.86$, $P < 0.01$].